DOUBLE POLARISATION IN NONLINEAR VIBRATING PIANO STRINGS

Jin Jack Tan, Cyril Touzé, Benjamin Cotté

IMSIA,
Institute of Mechanical Sciences and Industrial Applications,
ENSTA-ParisTech - CNRS - EDF - CEA,
Université Paris-Saclay,
828 Boulevard des Marchaux, 91762 Palaiseau Cedex, France
jtan@ensta.fr

ABSTRACT

The present work studies the double polarisation phenomenon observed in vibrating piano strings. From the experimental viewpoint, it is known that when a string is given an initial displacement in one transverse direction (e.g. hammer excitation in the vertical plane), the second transverse displacement (e.g. in the horizontal plane) is also excited after a few milliseconds and the amplitude can be of similar order to the first transverse displacement. This phenomenon contributes to a characteristic piano sound feature called the "double decay". The purpose of this study is to investigate the role of nonlinearities in inducing double polarisations. The nonlinear vibrations of the strings are studied with a two-degrees-of-freedom (dofs) system extracted from the Kirchhoff-Carrier string equations. The method of multiple scales is used to study the free vibrations of two polarisations having nearly equal eigenfrequencies and thus presenting a 1:1 internal resonance. For an imperfect string with slightly different eigenfrequencies between the two polarisations, it is found out that depending on the energy of the excitation, an uncoupled transverse mode can develop into a coupled mode where there is energy exchange between the two transverse polarisations. The coupled mode is stable and the string oscillates in an elliptic path. Numerical experiments are also carried out, confirming the findings of the analytical approach.

1. INTRODUCTION

This study on the double polarisation of piano strings is contained in a larger project which aims at developing a physically-based time-domain piano sound synthesis model. The work was pioneered by Chabassier [1] who proposed a refined complete model of a grand piano [2, 3]. However a few points still need additional developments. For example, one tonal feature that was not observed in the simulated sound is the double decay, i.e. where the temporal signal exhibits two envelopes with different decay rates. It is understood that one of the contributing factors of double decay is the double polarisation of piano strings, as first reported by Weinreich [4]. The double polarisation phenomenon is not modeled in Chabassier's work which may explain the absence of double decay in her modeled piano sound. The double polarisation can be caused by various factors, such as nonlinearities of piano strings, asymmetry and complex boundary conditions, coupling to unison strings etc. [5, 6, 7, 8, 9].

In this contribution, we focus on the nonlinearity experienced by piano string vibrating at large amplitudes as a possible cause for explaining the birth of double polarisation. More particularly the two fundamental eigenfrequencies of a string

with double polarisation are known to have close values, thus showing a 1:1 internal resonance. It is also known from other studies on nonlinear vibrations [10, 11] that thanks to a 1:1 internal resonance, energy can be exchanged between vibration modes so that even if the motion is initiated along one polarisation only, the nonlinearity can make this motion unstable, so that eventually a coupled vibration arises with the two polarisations involved. The objective of the present contribution is thus to clearly establish if the nonlinearity can be the cause of this coupling, as well as to highlight the main parameters governing the transfer of energy. The 1:1 internal resonance has already been studied in the case of forced vibrations, see *e.g.* [12, 10, 11]. Here our interest is in the case of free vibration for which only Manevitch and Manevitch present a detailed investigation [13]. The complete problem will hence be fully revisited and applied to the specific case of strings.

The article is organised as follows. First, a system of nonlinear Kirchhoff-Carrier string equations is presented in section 2 and solved via the multiple scales method in section 3. The results are presented and discussed in section 4. The paper continues with a numerical experiment to demonstrate the double polarisations in section 5 before wrapping up with conclusion in section 6.

2. KIRCHHOFF-CARRIER EQUATION

The Kirchhoff-Carrier equations for a freely vibrating fixed-fixed string with two polarised displacements u_1 and u_2 read [14, 15, 11]:

$$\rho A \ddot{u}_1 - (T_0 + N) u_1'' = 0, \tag{1a}$$

$$\rho A \ddot{u}_2 - (T_0 + N) u_2'' = 0, \tag{1b}$$

where N is the axial tension created by the large amplitude motions and the coupling with the transverse motion. It reads:

$$N = \frac{EA}{2L} \int_0^L \left(u_1'^2 + u_2'^2 \right) \, \mathrm{d}x. \tag{2}$$

In this set of equations, L is the length, A the crosse section area, E Young's modulus, T_0 the tension and ρ the density. Among others, underlying assumptions are that the inertia of the longitudinal component is negligible, see *e.g.* [16, 14] for more details. Following [11], the equations can be made nondimensional for a more general treatment.

The solutions of the nondimensional equations can be ex-

pressed in modal form:

$$u_1(x,t) = \sum_{k=1}^{K} \Phi_k(x)p_k(t), \qquad u_2(x,t) = \sum_{k=1}^{K} \Phi_k(x)q_k(t),$$
(3)

where $\Phi_k(x)$ are the mode shapes, and $\{p_k(t), q_k(t)\}_{k \geq 1}$ the modal coordinates. Restraining only the fundamental mode in the truncation for each polarisation (*i.e.* $K = 1$) and using the usual projection (Galerkin) technique, on obtains the following two dofs nonlinear system for the two modal coordinates p, q related to each polarisation:

$$\ddot{p} + \omega_1^2 p + \varepsilon \left[\Gamma_1 p^3 + C_1 p q^2 \right] = 0, \qquad (4a)$$

$$\ddot{q} + \omega_2^2 q + \varepsilon \left[\Gamma_2 q^3 + C_2 q p^2 \right] = 0, \qquad (4b)$$

where ε is a small parameter arising from the nondimensionalisation [11], $\varepsilon = EAd^2/T_0 L^2$, with d the diameter of the string. For a perfect string, the two eigenfrequencies are equal so that $\omega_2 = \omega_1 = \pi$ [11]. The same holds for the nonlinear coefficients, in a perfect case we have $\Gamma_1 = \Gamma_2 = C_1 = C_2 = \pi^4/2$. However, acknowledging that such perfect string does not exist in reality, a detuning parameter σ_1 is introduced so that the two eigenfrequencies of the two modes are possibly slightly different,

$$\omega_2 = \omega_1 + \varepsilon\sigma_1. \qquad (5)$$

Following the same lines, the system will be studied with general and different nonlinear coefficients so as to draw the complete picture for the nonlinear string. In a given experimental case, a procedure would be needed for identifying these coefficients.

3. MULTIPLE SCALES METHOD

The system in equation (4) is solved by the multiple scales method which describes the original system to be function of multiple independent time scales. Introducing the "fast" and "slow" time scales:

$$T_0 = t, \qquad (6a)$$

$$T_1 = \varepsilon t, \qquad (6b)$$

p and q can take the following form,

$$p(t) = p_0(T_0, T_1) + \varepsilon p_1(T_0, T_1) + O(\varepsilon^2), \qquad (7a)$$

$$q(t) = q_0(T_0, T_1) + \varepsilon q_1(T_0, T_1) + O(\varepsilon^2), \qquad (7b)$$

where p_0 and q_0 can be written as:

$$p_0 = A(T_1)\exp(i\omega_1 T_0) + c.c, \qquad (8a)$$

$$q_0 = B(T_1)\exp(i\omega_2 T_0) + c.c, \qquad (8b)$$

where $c.c$ stands for complex conjugates. A and B are unknown complex functions of T_1. Substituting equation (7) into (4) and grouping all the resonant terms for 1:1 resonance up to order ε, one obtains the solvability conditions. By writing A and B in polar form:

$$A(T_1) = a(T_1)\exp(i\alpha(T_1)), \qquad (9a)$$

$$B(T_1) = b(T_1)\exp(i\beta(T_1)), \qquad (9b)$$

the solvability conditions can be broken down into a set of four dynamical equations (two for amplitude a and b, two for the

phases α and β):

$$a' = -\frac{C_1}{2\omega_1}ab^2\sin(\gamma_2 - \gamma_1), \qquad (10a)$$

$$\gamma_1' = \frac{3\Gamma_1}{\omega_1}a^2 + \frac{C_1}{\omega_1}b^2\left[2 + \cos(\gamma_2 - \gamma_1)\right], \qquad (10b)$$

$$b' = \frac{C_2}{2\omega_2}ba^2\sin(\gamma_2 - \gamma_1), \qquad (10c)$$

$$\gamma_2' = \frac{3\Gamma_2}{\omega_2}b^2 + \frac{C_2}{\omega_2}a^2\left[2 + \cos(\gamma_2 - \gamma_1)\right] + 2\sigma_1, \qquad (10d)$$

where

$$\gamma_1 = 2\alpha, \qquad \gamma_2 = 2\beta + 2\sigma_1 T_1. \qquad (11)$$

The introduction of equation (11) is necessary so that the system is made autonomous (not directly dependent on any time scales).

3.1. Uncoupled solutions

Let us first consider the uncoupled solutions. They correspond to the motions of the strings that are either in the horizontal direction, or in the vertical one. The first set of uncoupled solutions is found by setting $b = 0$, in Eqs. (10). The 4-dofs system then degenerates into a two dofs and reads:

$$a' = 0, \qquad (12a)$$

$$\gamma_1' = \frac{3\Gamma_1}{\omega_1}a^2, \qquad (12b)$$

The equations can be easily integrated to give:

$$a = C_a, \qquad (13a)$$

$$\alpha = \frac{3\Gamma_1}{2\omega_1}a^2 T_1 + \alpha_a, \qquad (13b)$$

where C_a and α_a are both integration constants independent of T_1. Using this result, the solution p_0 can be expressed as:

$$p_0 = 2a\cos\left[\omega_{NL}t + \alpha_a\right], \qquad (14)$$

where

$$\omega_{NL} = \omega_1\left(1 + \varepsilon\frac{3\Gamma_1}{2\omega_1^2}a^2\right). \qquad (15)$$

The first order solution is thus a periodic orbit where only p is involved in the vibration since setting $b = 0$ implies $q = 0$. The nonlinear frequency of oscillation ω_{NL} depends on the amplitude a, a usual feature in nonlinear oscillations. For a positive value of Γ_1, which is the case for strings, the nonlinearity is of the hardening type, *i.e.* the oscillation frequency increases with the amplitude.

A similar exercise can be done for the other uncoupled case, i.e. $a = 0$ and one would obtain a similar result for q_0,

$$q_0 = 2b\cos\left[\omega_{NL}t + \beta_b\right] \qquad (16)$$

where

$$\omega_{NL} = \omega_2\left(1 + \varepsilon\frac{3\Gamma_2}{2\omega_2^2}b^2\right) \qquad (17)$$

One can notice the similarity between the two solutions, coming from the fact that the uncoupled solutions are ruled out by classical Duffing equations. The nonlinearity is completely governed by coefficients Γ_1 and Γ_2. Figure 1 shows the backbone curve (amplitude-frequency relationship, Eqs. (15)-(17)) for $\varepsilon = 0.163$, a typical value for a string that has been computed using standard values from [1]. The value $\Gamma = 0$ is used
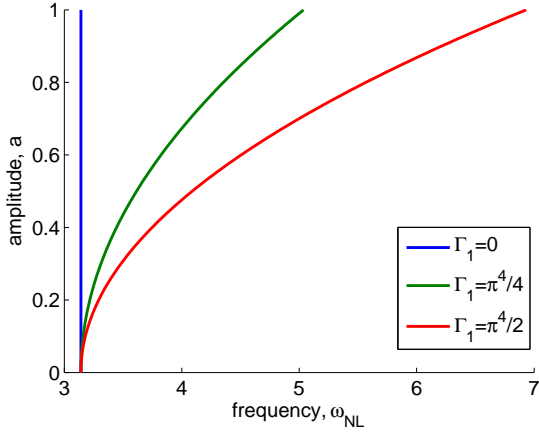
Figure 1: Relationship between a and ω_{NL} for various Γ_1 at $\omega_1 = \pi$, $\varepsilon = 0.163$.

as an eyeguide to recall that for linear vibrations, the oscillation frequency is independent from the amplitude. The values $\Gamma = \pi^4/2$, $\omega = \pi$ are the standard values for perfect strings. Finally $\Gamma = \pi^4/4$ is plotted as an intermediate case between the linear string and the perfect nonlinear string. The figure allows one to estimate the deviation (in radian frequency) of the oscillations with respect to the linear eigenfrequency, as a function of the vibration amplitude.

3.2. Coupled solutions

Let us now investigate the coupled solutions of the conservative system given by Eqs. (10). Stationary oscillations occurs at a given energy level so that coupled solutions can be searched for fixed amplitudes, by imposing $a' = b' = 0$. This is also in the line of the uncoupled cases where periodic solutions were found for fixed amplitudes and only phase variations, from which the nonlinear amplitude-frequency relationship were derived. From equation (10a) and (10c), it is obvious that for coupled solutions to exist (i.e. $a \neq 0$, $b \neq 0$), one must have mandatory $\sin(\gamma_2 - \gamma_1) = 0$. This implies in particular that $\cos(\gamma_2 - \gamma_1) = \pm 1$. Interestingly, for each case of the possible value of the cosine, the two polarisations p and q are related in a different manner. For $\cos(\gamma_2 - \gamma_1) = +1$, a simple algebra on the system shows that the solutions p and q are related by the following relationship:

$$\frac{q}{p} = \pm\frac{b}{a}, \tag{18}$$

while for $\cos(\gamma_2 - \gamma_1) = -1$, p and q are related by:

$$\frac{q^2}{4b^2} + \frac{p^2}{4a^2} = 1. \tag{19}$$

These particular forms expressed by the coupled solutions has already been commented by Manevitch and Manevitch [13], who refers to them respectively as "normal mode" (NM) (former case, Eq. (18)), and "elliptic mode" (EM) (latter case, and Eq. (19)). This peculiar relationship expressed for each time between the solution amplitudes leads to a particular motion which is sketched in Figure 2 in the (p, q) (displacements) plane. The elliptic mode appears particularly interesting for us as it corresponds to the whirling motion observed in piano strings [9].

The nonlinear amplitude-frequency relationships defining the backbone curves for coupled solutions can be found out
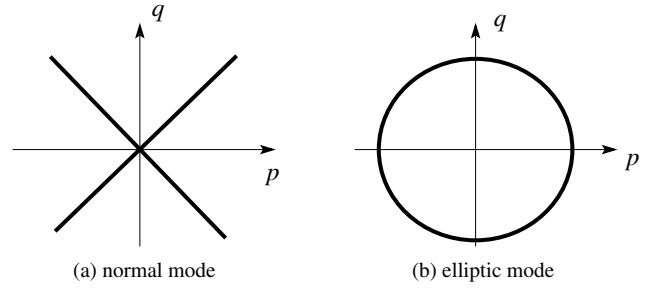

Figure 2: Illustrations of the two modes of coupled solutions. Image not to scale.

by setting $\cos(\gamma_2 - \gamma_1) = \pm 1$ in Eqs. (10b)-(10d), where the right-hand sides become constants, so that one can retrieve α, β and subsequently the nonlinear frequency ω_{NL} for the coupled modes as:

$$\omega_{NL} = \omega_1 \left[1 + \varepsilon \left(\frac{3\Gamma_1}{2\omega_1^2}a^2 + \frac{rC_1}{2\omega_1^2}b^2\right)\right]. \tag{20}$$

In this equation (and in the remainder of the article), the parameter r is such that $r = 3$ for normal mode, and $r = 1$ for elliptic modes respectively. As can be seen in equation (20), the nonlinear frequency is influenced by the amplitude of both polarisations a and b. The equation forms a surface on the 3D space defined by (a, b, ω_{NL}). However curved line solutions are awaited instead of a whole surface family. Noting that $\gamma_2 - \gamma_1 = n\pi$ from the necessary conditions of existence for coupled solutions, one has thus $\gamma_2' - \gamma_1' = 0$. Using such relation, one can obtain:

$$\left[\frac{rC_1}{\omega_1} - \frac{3\Gamma_2}{\omega_2}\right]b^2 + \left[\frac{3\Gamma_1}{\omega_1} - \frac{rC_2}{\omega_2}\right]a^2 = 2\sigma_1. \tag{21}$$

This relationship expresses the link between the amplitudes a and b for both normal ($r = 3$) and elliptic ($r = 1$) coupled modes. The conjuction of Eqs (20) and (21) define the backbone curves for the coupled modes.

Let us now investigate how the coupled solutions can be related to the uncoupled ones. By setting $a = 0$ or $b = 0$ in Eq. (21), it can be seen that either of the uncoupled modes can branch into the coupled modes provided the following conditions are met:
For uncoupled mode $a \neq 0$

$$a^2 \geq \frac{2\sigma_1}{\frac{3\Gamma_1}{\omega_1} - \frac{rC_2}{\omega_2}}, \tag{22}$$

For uncoupled mode $b \neq 0$

$$b^2 \geq \frac{2\sigma_1}{\frac{rC_1}{\omega_1} - \frac{3\Gamma_2}{\omega_2}}, \tag{23}$$

These equations provide a limit value, in terms of amplitudes of the uncoupled modes, for which the coupled solutions can develop. Below these limit value, only uncoupled solutions exist. It must be noted that in certain cases, the RHS of both the equations can have two positive values of which the lower one indicates the bifurcation point where the uncoupled solution branches into the coupled solution while the higher one indicates the point where the coupled solution collapse and enter the uncoupled solution [13].

3.3. Stability analysis

To obtain the stability of the coupled modes, Eqs (10) can be reduced to a 3-DOF system by taking the difference between the two phases or even further to a 2-DOF system as demonstrated by Manevitch and Manevitch [13]. The advantage of using such an approach is that the coupled solutions are then real fixed points of the 3- or 2-dofs systems, so that the usual tools from dynamical system theory can be used for investigating stability. One can thus construct the Jacobian matrix of the corresponding system and solve for the eigenvalues. Using either system will result in the same following stability criteria for the coupled modes:

$$\frac{\omega_2 \Gamma_1}{C_2 \omega_1} + \frac{\Gamma_2 \omega_1}{C_1 \omega_2} < 2 \qquad \text{for normal modes,} \qquad (24a)$$

$$\frac{\omega_2 \Gamma_1}{C_2 \omega_1} + \frac{\Gamma_2 \omega_1}{C_1 \omega_2} > \frac{2}{3} \qquad \text{for elliptics modes.} \qquad (24b)$$

It is interesting to see that the stability of the coupled solutions does not depend on the energy but rather on the physical parameters of the system (i.e. eigenfrequencies and nonlinear constants). It also means that regardless of level of excitation, exhibition of stable normal or elliptic modes are pre-determined.

To conclude the analytical study, let us investigate the stability of uncoupled solutions and demonstrate how uncoupled solutions can become unstable in favour of a coupled one. As noted by Manevitch and Manevitch [13], the stability of the uncoupled solutions is determined by the energy of the system. Using the same approach as for the coupled case does unfortunately not give a useful criteria for the stability of uncoupled solutions, which are found to be always unstable. Furthermore, Manevitch and Manevitch do not give an explicit proof of the stability of uncoupled solutions in [13]. The underlying problem is that when setting either $b = 0$ or $a = 0$ in the system, the degeneracy is ill-conditioned so that the phase space shrinks down to a two dofs system where the perturbation brought by the other oscillators are not defined and thus cannot be studied. The solution is found from the forced and damped vibration cases by canceling the damping terms and identifying the external excitation frequency to the nonlinear oscillation frequency ω_{NL}. Using the existence conditions derived in [10] from a geometric analysis in phase space, one can obtain the following *instability regions* for the uncoupled solutions:
For uncoupled mode $a \neq 0$

$$\omega_{NL} = \omega_2 + \varepsilon r \frac{C_2}{2\omega_2} a^2 \qquad (25)$$

For uncoupled mode $b \neq 0$

$$\omega_{NL} = \omega_1 + \varepsilon r \frac{C_1}{2\omega_1} b^2 \qquad (26)$$

where $r = 1$ and $r = 3$ define the lower and upper bound of the instability region, that are simply related to the connection with either elliptic mode or normal mode. The instability affecting the uncoupled mode $a \neq 0$ originates from the eigenfrequency of the other uncoupled mode, ω_2 and vice versa. This is because the existence of another uncoupled solution upsets the stability of the original uncoupled solution. It is also interesting to note that the point where the uncoupled solution changes its stability (either in losing or restoring it) is also the point where the uncoupled solution branches into a coupled solution (or a coupled solution leaves and enters the uncoupled solution). Finally, the stability of the uncoupled solutions are seen to depend on the coupling nonlinear coefficients C_1 and C_2 only, as can be expected.
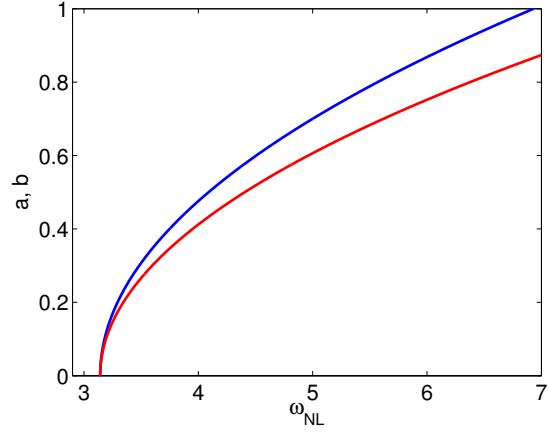
4. RESULTS AND DISCUSSIONS

Figure 3: Amplitude-frequency relationships for the strings, perfect case with $\omega_1 = \omega_2 = \pi$ (no detuning: $\sigma_1 = 0$), and equal nonlinear coefficients $C_1 = C_2 = \Gamma_1 = \Gamma_2 = \pi^4/2$. The black ▬ and blue ▬ lines (overlapped with each other) indicate the two uncoupled modes while the red ▬ line indicates the elliptic mode. $\varepsilon = 0.163$.

In this section, several case studies are made to demonstrate the properties of the system. Firstly, a perfect string case is considered (i.e. $\sigma_1 = 0$, $C_1 = C_2 = \Gamma_1 = \Gamma_2$). For this case, the two amplitude-frequency relationships for uncoupled solutions given by Eqs. (15) and (17) are exactly the same so that the backbones in Fig. 3 collapse on the same curve (black and blue curves, only the blue being visible). For the coupled solutions, Eqs. (21) for the normal mode ($r = 3$) degenerates, indicating that no normal modes are possible in the perfect case. On the other hand, elliptic modes does however exist, and Eqs. (21) shows that they have same amplitude : $a = b$. Reporting in Eq. (20), one obtains the backbone curve for the coupled, ellipitc modes in the perfect case as: $\omega_{NL} = \omega_1(1 + 2\varepsilon \frac{\Gamma_1}{\omega_1} a^2)$. This shows that coupled solutions have a stronger hardening behaviour than uncoupled ondes, as reported in Fig. 3 with a red line. It must be noted that a 2D representation has been chosen for simplicity, by using the same axis for both amplitudes a and b, whereas the whole solutions should be plotted in a 3D space. In such 3D space (a, b, ω_{NL}), uncoupled solutions are restricted respectively to the planes (a, ω_{NL}) and (b, ω_{NL}), whereas the coupled elliptic solutions is in the plane $a = b$.

Finally, examining the different stability conditions found in the previous section for both coupled and uncoupled modes leads to the conclusion that all the solutions reported in Fig. 3 are stable. This leads to the important conclusion that if the motion is excited on a given polarization, then it will stay on it for every time so that no whirling motion of the string would be observed. The coupled elliptic solutions could be observed only if very specific initial conditions are given to the string so that the motion is initiated along this mode.

Let us now turn to the more realistic case of an imperfect string. The most simple imperfection with a slight detuning between the two eigenfrequencies of the polarisation is investigated, by setting $\sigma_1 = 1$, and keeping all the nonlinear coupling coefficients equal: $C_1 = C_2 = \Gamma_1 = \Gamma_2$. The backbone curves are represented in Fig. 4, where now the two uncoupled solutions (black and blue lines) are different and originates respectively from ω_1 and $\omega_2 = \omega_1 + \varepsilon\sigma_1$. Eqs (21) shows once again
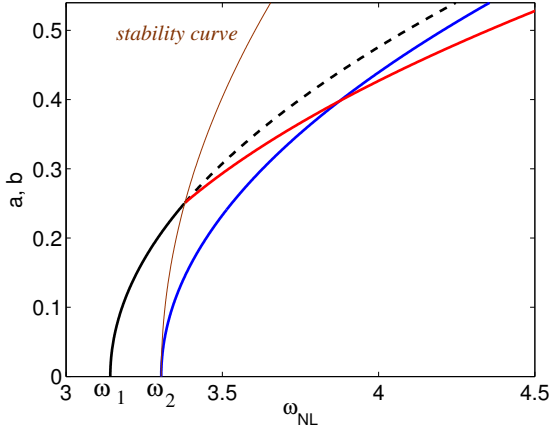
Figure 4: Amplitude-frequency relationships for periodic solutions of the nonlinear string, imperfect case with $\sigma_1 = 1$, all other coefficients being the same as in Fig. 3: $C_1 = C_2 = \Gamma_1 = \Gamma_2 = \pi^4/2$, $\omega_1 = \pi$, $\varepsilon = 0.163$. Black ▬ : uncoupled solution $a \neq 0$, blue ▬ uncoupled solution $b \neq 0$, red ▬ coupled elliptic mode. Dashed lines ‑ ‑ indicates instability. In brown is given the instability limit predicted by Eq. (25).

that in this case normal modes are not likely to exist. Only elliptic modes are possible. The instability condition for uncoupled solutions, provided by Eq. (25)-(26), shows that:

- The uncoupled solutions with $b \neq 0$ are always stable.

- On the other hand, uncoupled solutions with $a \neq 0$ can be unstable and branch on an elliptic mode, recovering also the criteria given by Eq. (22).

The instability region for uncoupled mode with $a \neq 0$ given by Eq. (25) has two curves. The one for normal mode ($r = 3$) is not relevant. Finally only the instability line with $r = 1$ is meaningful, and is represented as a brown line in Fig. 4. The crossing between the sdof uncoupled solution and the instability limit occurs exactly when condition (22) is fulfilled. From this point, uncoupled solutions are unstable, and the branch of elliptic mode solutions (red line) emerges. Once again a 2D representation has been chosen for simplicity, the reader must however keep in mind that the red line is neither in the plane (a, ω_{NL}), nor in (b, ω_{NL}), but really develop in the full 3D space and is not contained within a plane. In particular the crossing between the coupled solution (red line) and uncoupled ($b \neq 0$, blue curve) is only a matter of the representation used but does not exist in the full 3D space.

The important conclusion that can be drawn from this study is that as soon as an imperfection is taken into account, an unstable region in the backbone curve for uncoupled modes exist. Once the limit amplitude exceeded, uncoupled solutions are unstable so that even though an initial condition is given for that polarisation, an energy transfer will occur so that eventually the system would settle on the stable elliptic mode. Interestingly, one can notice from Eq. (25) that the smallest the detuning σ_1, the smallest the amplitude limit for unstable solutions occurs. Hence in order to observe easily this phenomenon, the detuning need not be zero, but should be as small as possible.

5. NUMERICAL EXPERIMENTS

The main analytical findings of the previous section is now compared to direct numerical simulations of the original system

given by Eqs. (4). More particularly, the mots interesting case of the imperfect string is considered, with a slight detuning between the two eigenfrequencies of the two polarisations. The equations of motion are directly integrated numerically in time with a fourth-order Runge-Kutta method. The experiment is carried out with varying level of initial excitation on the first mode only, mimicking the case of a piano string being struck with a hammer of increasing velocities, and hence exciting the string in only one polarisation. The values of the case previously studied in Fig. 4 are selected. The analytical study predicts that the uncoupled solution should be stable as long as $a < 0.25$. A first case is thus studied below this limit value, with an initial condition in displacement only, with $p(t = 0) = 0.4$ and $q(t = 0) = 1e - 4$. Note that, from Eqs. (9)-(14), a factor 2 between a (resp. b) and the amplitude solution in time for $p(t)$ (resp. $q(t)$), is present, so that the limit amplitude for stability for $p(t = 0)$ is 0.5. The direct time integration is represented in Fig. 5. One can observe that below the amplitude where instability occurs, the second coordinate $q(t)$ stays at negligible values around $1e - 4$.
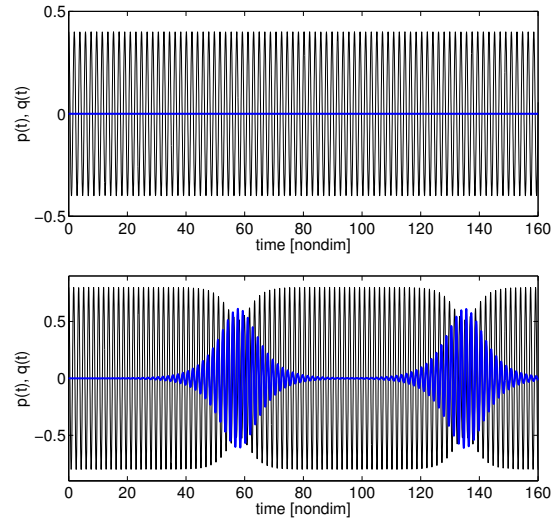

Figure 5: Time responses from direct numerical integration of Eqs. (4) and for varying levels of initial displacements $p(t = 0)$. At the top, $p(t = 0) = 0.4$, below the instability limit; at the bottom, $p(t = 0) = 0.8$, above the instability limit. Black ▬ line correspond to $p(t)$ and blue ▬ line to $q(t)$.

For an initial condition above the instability limit, $p(t = 0) = 0.8$, one can observe that an energy exchange between the two modes occurs and $q(t)$ reaches values up to 0.6. The energy then gets back and forth between the two oscillators, a typical feature of nonlinear conservative oscillations [12]. This numerical experiment confirms the instability of the uncoupled solution. It also shows that, for a given piano string, and for amplitude of excitation that are above a certain threshold that can be predicted, a motion initiated along a single polarisation can be transformed into a coupled whirling motion, as observed experimentally.

6. CONCLUSION

A detailed study has been conducted to examine the two polarisations of nonlinear vibrating strings, and to show if the geometric nonlinearity due to large-amplitude vibration can be responsible of the coupling between the two polarizations, even

though the motion is initiated along a single direction. An analytical study has been conducted using a two-modes approximation for the Kirchhoff-Carrier equation, and then the method of multiple scales. The frequency-amplitude relationships of the two polarisations and the ways whirling motion can take place are identified. The main finding of the anlytical study reveals that an imperfection is needed in order to make uncoupled solutions unstable. When all the coefficients are equal, in the mathematical case of a perfect string, then the periodic solutions are all stable. When a detuning is considered between the two eigenfrequencies, which is always the case in practice, then uncoupled solutions can become unstable and whirling motions of the string can take place even though the motion is initiated along one polarisation only. These results also clearly demonstrate that the geometric nonlinearity can be a potential cause for the whirling motions observed in real piano strings. Future work will consider experimental validations of these findings. The imperfections brought by the specific boundary conditions of the piano string will also be studied in order to assess their role in the appearance of double polarisation.

7. ACKNOWLEDGEMENT

8. REFERENCES

[1] J. Chabassier, *Modélisation et simulation numérique d'un piano par modèles physiques*, Ph.D. thesis, École Polytechnique, 2012.

[2] J. Chabassier, A. Chaigne, and P. Joly, "Time domain simulation of a piano. Part 1 : model description.," *ESAIM: Mathematical Modelling and Numerical Analysis*, vol. 48, no. 05, pp. 1241–1278, 2013.

[3] J. Chabassier, P. Joly, and A. Chaigne, "Modeling and simulation of a grand piano," *Journal of the Acoustical Society of America*, vol. 134, pp. 648, 2013.

[4] G. Weinreich, "Coupled piano strings," *J. Acoust. Soc. Am.*, vol. 62, pp. 1474, 1977.

[5] T. C. Hundley, H. Benioff, and D. W. Martin, "Factors contributing to the multiple rate of piano tone decay," *J. Acoust. Soc. Am.*, vol. 64, no. 5, 1978.

[6] H. Suzuki and I. Nakamura, "Acoustics of pianos," *Applied Acoustics*, vol. 30, pp. 147, 1990.

[7] J. Burred, *The acoustics of the Piano*, Ph.D. thesis, Professional Conservatory of Music Arturo Soria, 2004.

[8] C. Karatsovis, *Acoustic Features of Piano Sounds*, Ph.D. thesis, University of Southampton, 2011.

[9] A. Chaigne, J. Chabassier, and N. Burban, "Acoustics of pianos: physical modeling, simulations and experiments," in *Proceedings of SMAC 2013, Stockholm, Sweden*, 2013.

[10] C. Touzé, O. Thomas, and A. Chaigne, "Asymmetric nonlinear forced vibrations of free-edge circular plates. part I: Theory," *Journal of Sound and Vibration*, vol. 258, pp. 649–676, 2002.

[11] O. Thomas, A. Lazarus, and C. Touzé, "A harmonic-based method for computing the stability of periodic oscillations of non-linear structural systems," in *Proceedings of the ASME 2010 IDETC conference, Montreal, Canada*, 2010.

[12] A.H. Nayfeh and D.T. Mook, *Nonlinear Oscillations*, Wiley, 1979.

[13] A. Manevitch and L. Manevitch, "Free oscillations in conservative and dissipative symmetric cubic two-degree-of-freedom systems with closed natural frequencies," *Meccanica*, vol. 38, pp. 335–348, 2003.

[14] S. Bilbao, "Conservative numerical methods for nonlinear strings," *The Journal of the Acoustical Society of America*, vol. 118, no. 5, pp. 3316–3327, 2005.

[15] T. Hélie and D. Roze, "Sound synthesis of a nonlinear string using volterra series," *Journal of Sound and Vibration*, vol. 314, no. 12, pp. 275 – 306, 2008.

[16] P. Morse and U. Ingard, *Theoretical Acoustics*, Princeton University Press, 1968.